

Dielectric studies of ferroelectric liquid crystals ^a

Iwao Teraoka, Richard L. Siemens, Robert J. Twieg and Kathleen Betterton
IBM Research, 650 Harry Road, San Jose, CA 95120-6099 (USA)

(Received 17 May 1991)

Abstract

The dielectric properties of some ferroelectric alpha-chloroester thiobenzoate liquid crystal materials have been studied using a Du Pont 2970 dielectric analyzer (DETA) in the 0.01 Hz–100 kHz range. These materials exhibit smectic A and chiral smectic C mesophases, as well as additional mesophases in some cases. Transitions involving the chiral smectic C phase are of most interest because this phase has ferroelectric properties. The effect on these transitions of fluorine addition to the alkoxy tail was investigated. The Goldstone mode and soft mode are seen in the frequency dispersion curves of the dielectric loss factor.

Very low heating rates of $0.01^{\circ}\text{C min}^{-1}$ and small step-wise increments are possible, providing measurements at small temperature increments which permit close observation of the transition regions. DSC measurements and optical microscopy observations were also performed and the three techniques were found to be complementary.

INTRODUCTION

There is a growing interest in ferroelectric liquid crystal (FLC) materials with promising applicability to fast-switching optical and display devices. FLC molecules usually have a structure of a rigid-rod core with a chiral carbon and a flexible tail. The chiral carbon is located close to a permanent dipole moment perpendicular to the director axis. A variety of FLC usually has isotropic (I), smectic A (SmA), chiral smectic C (SmC*), and crystalline (K) phases obtained on cooling, with some occasional additional mesophases or subphases. An exothermic peak is expected in the DSC measurement at every transition temperature. However, the peak is not always clearly observed because an enthalpy change at the transition can be comparable to a component of specific heat at usual heating rates. In particular, the phase transition from SmC* to SmA is often difficult to observe. One of the differences between these two phases is that the SmC* phase has a correlation in the orientation of the permanent dipole moments (ferroelectric), while the SmA phase does not (paraelectric). Therefore, we can expect a large change in the dielectric properties around the phase transition. The

^a Presented at the 19th Annual NATAS Conference, Boston, MA, 23–26 September 1990.

present report focuses on the SmA to SmC* phase transition on cooling as studied by dielectric relaxation spectroscopy. We will demonstrate that the dielectric analysis can be a powerful tool to investigate the transition temperature as well as the anomalous dielectric behaviors at the transition and throughout the SmC* phase.

Studies of the frequency dispersion of dielectric relaxation around the SmA to SmC* transition to date have focused on the standard FLC material DOBAMBC and some commercially available FLC mixtures which exhibit SmC* phase at room temperature [1]. These FLC materials have been found to have two modes of dipolar motion in the SmC* phase. The high-frequency soft mode involves fluctuation of the tilt angle (polar angle of the director with smectic layer normal the polar axis), and the low-frequency Goldstone mode is ascribed to fluctuation of the azimuthal angle of the director around the layer normal (winding-unwinding motion of the director). Studies to date have also discovered critical anomalies with a rapid increase of the dielectric increment and slowing down of the soft mode. However, the mechanism involved in the SmA to SmC* phase transition has yet to be studied intensively. The SmA to SmC* transition is believed to involve an onset of correlation in directions of the permanent dipole moments as well as non-zero tilt angle. There is a report that these two order parameters, depending on the structure of FLC molecules, gain non-zero values at different temperatures in the cooling process [2].

SAMPLES

The ferroelectric liquid crystals studied here are members of a large set of thiobenzoate core α -haloester materials currently under examination as components of mixtures for high-speed optical modulators [3]. The thiobenzoate core is particularly useful in producing the requisite tilted smectic phases, and the chiral and polar chloroester tail is well known to provide large spontaneous polarizations in combination with many cores. Recently we have begun to modify the all-hydrocarbon $\text{H}(\text{CH}_2)_m\text{O}-$ achiral tails by the systematic replacement of hydrocarbon by blocks of fluorocarbon to produce semi-fluorinated tails, $\text{F}(\text{CF}_2)_n(\text{CH}_2)_m\text{O}-$. The total length of the tail ($n + m$) and the ratio (n/m) of the segments has a dramatic impact on the mesophase behavior, in some cases the ferroelectric phase ranges are broadened considerably. Figure 1 shows the molecular structures of the three FLC compounds studied here. They are designated as FLC(I), (II) and (III). The phase transition temperatures in the heating process observed by optical microscope are given in Table 1.

EXPERIMENTAL

The measurements were performed using a Du Pont 2970 dielectric analyzer in both the interdigitated or ceramic single surface (SS) and the

parallel plate (PP) electrode configurations. The SS sensor, with channels 12.5 μm deep and 125 μm long, was covered to a depth of approximately 1 mm. When using the PP sensor, the electrode separation was between 0.1 and 0.2 mm. These two electrode configurations combined provide an anisotropic dielectric constant of the FLC samples, that is molecularly aligned by the surface effect.

The applied voltage between the electrodes was 1 V. We employed mostly 25 frequencies located at equal interval in log scale from 0.1 Hz to 100 kHz, with the information on the relaxation modes coming from frequencies above 10 Hz. The data suppression capability was not used in order to facilitate plotting of the frequency dispersion curves showing the various relaxation modes.

Scan rates varied, but most of the work was done with very low scan rates around the phase transition, as low as 0.01 K min^{-1} , for both heating and cooling curves. The low rates provided temperature resolution as low as 0.02 K between two consecutive frequency dispersion measurements.

Data were transferred to our mainframe computer system in order to analyze the frequency dispersion data by a non-linear curve fitting program. The fitting equation for the complex dielectric constant ϵ^* at the frequency f is a Cole-Cole equation with a d.c. conductivity component:

$$\epsilon^* = \epsilon' - j\epsilon'' = \epsilon_\infty + \frac{\Delta\epsilon}{1 + (jf/f_r)^\alpha} + \frac{\sigma}{2\pi j\epsilon_0 f}$$

where ϵ' and ϵ'' are real and imaginary parts of ϵ^* , ϵ_∞ is the value of ϵ' at the high frequency limit, $\Delta\epsilon$ is the dielectric increment of the relaxation mode, f_r is the relaxation frequency, α is the broadening index (Cole-Cole index), σ is the d.c. conductivity, and ϵ_0 the vacuum permittivity. The Debye-type relaxation has $\alpha = 1$.

RESULTS AND DISCUSSION

In this report, we concentrate on the samples FLC(I) and FLC(III), the unfluorinated and the most fluorinated samples, respectively. FLC(II) showed dielectric behavior similar to that of FLC(III) except that the transition temperatures were different. In Fig. 2, the DSC result of FLC(I)

TABLE 1

Transition temperatures ($^{\circ}\text{C}$)

Material	K to SmC*	SmC* to SmA	SmA to I
FLC(I)	54.5	66	73.5
FLC(II)	91	(82)	107
FLC(III)	96	118	162

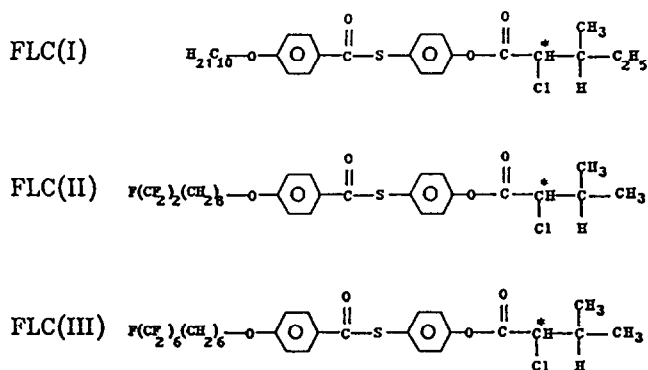


Fig. 1. Molecular structures of the three FLC compounds studied: FLC(I), (II), and (III).

measured in the heating run is shown by a solid line. We can see two major endothermic peaks at around 51.5°C (K to SmC*) and 71°C (SmA to I) and one small peak at around 63°C (SmC* to SmA). As expected, the endothermic peak at the phase transition from SmC* to SmA is hardly discernible. In the same figure, we overlapped the temperature dispersion of the dielectric constant ϵ' measured at 10 Hz with the SS electrode in the heating run. The value of ϵ' increases sharply at the K to SmC* transition, remains almost the same throughout the SmC* phase, and then drops sharply at the SmC* to SmA transition.

To examine more closely the dielectric properties at the SmA to SmC* transition in the cooling run, Fig. 3 shows the log-log plots of ϵ' and ϵ'' versus frequency measured with the SS electrode. We can see a sharp increase in the dielectric increment and a rapid shift of the peak frequency in the ϵ'' dispersion in a narrow temperature range at the transition. Only

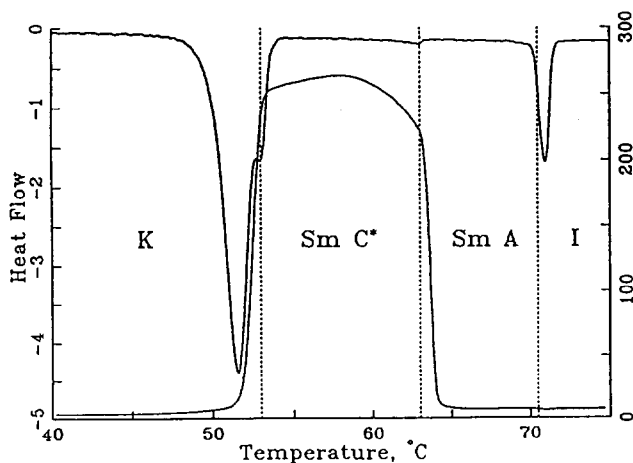


Fig. 2. DSC results of FLC(I), heating run, (solid line) shown with the temperature dispersion of the dielectric constant ϵ' measured at 10 Hz with the SS electrode.

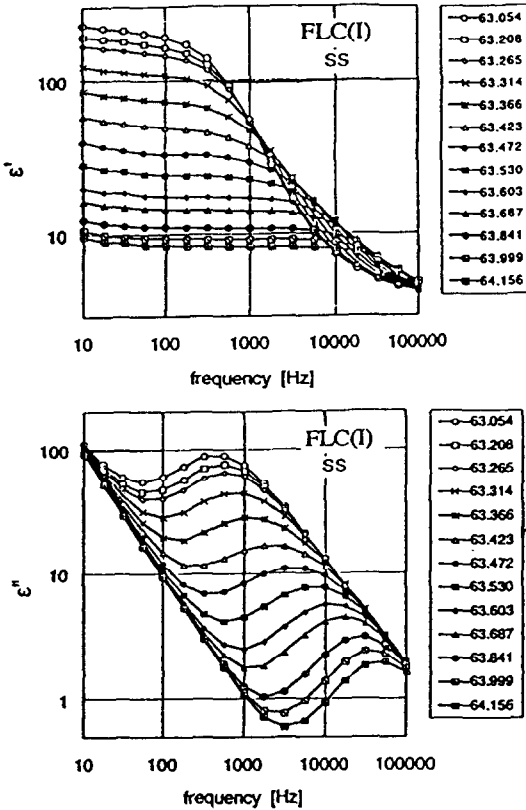


Fig. 3. Log-log plots of (left) ϵ'' and (right) ϵ' versus frequency for FLC(I) at the SmA to SmC* transition, in the cooling run, measured with the SS electrode.

one relaxation mode is observed in the frequency range of the present measurement (0.1 Hz–100 kHz) throughout the transition region and the SmC* phase. We performed non-linear curve fitting of the complex dielectric constant ϵ^* by the Cole-Cole equation plus d.c. conductivity. The best-fitted values of the dielectric increment $\Delta\epsilon$ and the relaxation frequency f_r are plotted in log scale against temperature in Fig. 4. Below 63°C, $\Delta\epsilon$ and f_r were almost unchanged with f_r being the typical relaxation frequency of the Goldstone mode. Plots of $1/\Delta\epsilon$ and f_r in linear scale follow straight lines above 63.5°C (SmA phase). These critical anomalies are also observed in other FLC materials such as DOBAMBC. They suggest that the number of molecules engaged in correlated motion increases as the temperature approaches the critical temperature from above (disordered phase). The observed relaxation mode is the same as the one explained as the slowing-down of the soft mode and its merging to the Goldstone mode in the SmC* phase.

On the other hand, the dielectric relaxation measured with PP electrodes (electrode spacing ≈ 0.2 mm) exhibited different characteristics. Two relaxa-

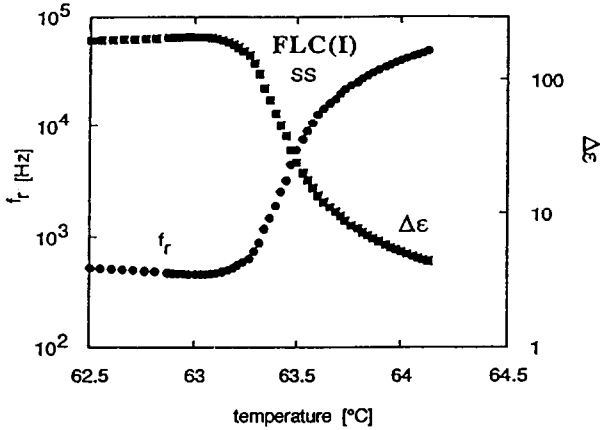


Fig. 4. The best-fitted values of the dielectric increment $\Delta\epsilon$ and the relaxation frequency f_r plotted in log scale against temperature.

tion modes ascribed to low-frequency and high-frequency were observed in the frequency dispersion over a wide range of temperature for the SmC^* phase. The dielectric increment was smaller than that measured with the SS electrode. The difference between the results measured with the two electrode configurations can be seen most distinctly in Fig. 5. The relaxation frequency of the high-frequency component obtained in the PP electrode measurement is plotted as a function of temperature together with that of the single relaxation mode in the SS electrode measurement. It appears that the relaxation modes observed in the PP electrode configuration can be ascribed to molecular motions independent of the SmA to SmC^* phase transition. More work is needed to confirm the validity of these conclusions and to exploit the different results obtained with the two configurations.

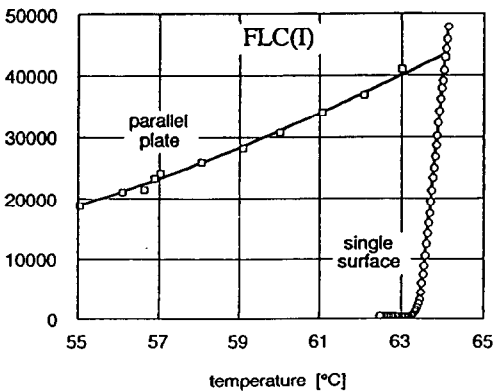


Fig. 5. The difference in the results as measured with the two electrode configurations for FLC(I) , SmC^* phase.

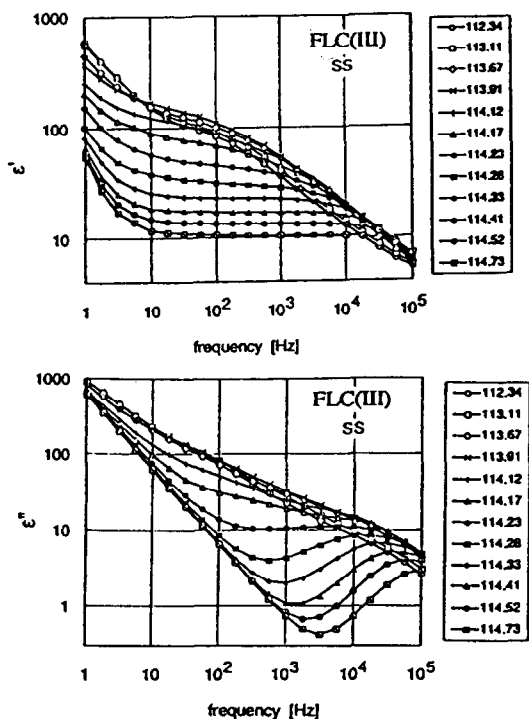


Fig. 6. Log-log plots of (left) ϵ' and (right) ϵ'' versus frequency for FLC(III) in the SmC* phase measured with the SS electrode.

For the other two FLC samples, FLC(II) and FLC (III), however, the Goldstone modes were not of the Cole-Cole type. Nor is the d.c. conductivity observed in the ϵ^* representation. Figure 6 shows the log-log plots of ϵ' and ϵ'' versus frequency for FLC(III) in the SmC* phase measured with the SS electrode. As the temperature is lowered from the SmA phase, the peak frequency in ϵ'' shifts rapidly to a lower frequency. In the SmC* phase, the spectrum becomes monotonic over the whole range of frequency, but the slope is not -1 as seen in conductive materials. The Goldstone modes in these materials should have an extremely extended range of relaxation frequency. The relaxation frequency in the SmA phase depends almost linearly on the temperature (Fig. 7). The transition behaviors of FLC(III) measured with PP electrodes are again very different from those measured with the SS electrode, as seen in Fig. 8.

In conclusion, measurement of the dielectric relaxation spectrum around the SmA to SmC* phase transition of FLC materials in a slow cooling process have uncovered interesting transition phenomena which are correlated with the dipole moments. Samples subjected to a strong surface effect exhibited a sharp transition for both unfluorinated and fluorinated thio-benzoate liquid crystals. The fluorinated samples showed the Goldstone

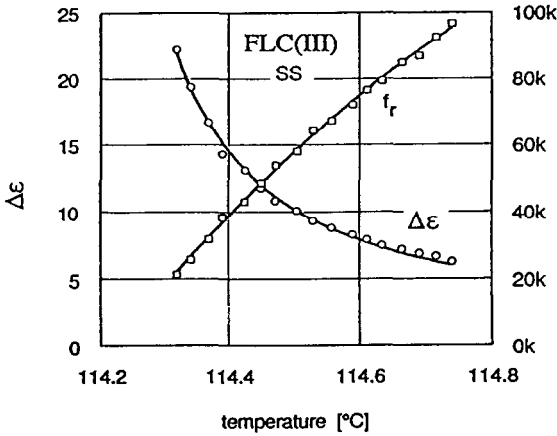


Fig. 7. The dielectric increment of the relaxation frequency $\Delta\epsilon$ and the relaxation frequency f_r plotted against temperature for FLC(III) measured with the SS electrode.

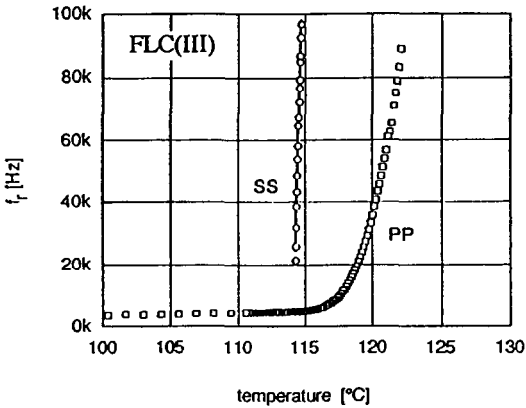


Fig. 8. The transition behaviors of FLC(III) as measured with the two electrode configurations.

mode with its characteristic frequency extremely extended over several orders of magnitude.

REFERENCES

- 1 C. Filipic, T. Carlsson, A. Levstik, B. Zeks, R. Blinc, F. Gouda, S.T. Lagerwall and K. Skarp, *Phys. Rev. A*, 38 (1988) 5833.
- 2 K. Hiraoka, A. Taguchi, Y. Ouchi, H. Takezoe and A. Fukuda, *Jpn. J. Appl. Phys.*, 29 (1990) L103.
- 3 R.J. Twieg, K. Betterton, H.T. Nguyen, W. Tang and W. Hinsberg, *Ferroelectrics*, 91 (1989) 243.